Electronic Supplementary Material (ESI) for New Journal of Chemistry.

Catalytic oxidative desulfurization performance of modified nano-sized β zeolite loaded with different structural polyoxometalates

Jinhong Li [a], Haonan Li[a], Zhimei Song[a], Ying Guo[a], Mengxiao Tai[a], Mei Han[a], Xinyao Wang[a], Lidong Chen *[a], Dongmei Ren*[b]

a. Faculty of Chemistry and Chemical Engineering, Liaoning Normal University, Dalian, 110629, Liaoning, PR China

b. College of Chemistry and Chemical Engineering, Bohai University, Jinzhou, 121013, PR China

2.1. Materials

Table. S1 Primary materials in the experiment

Chemicals	Chemical formula	Purity	Sources of Chemicals
Tetraethyl orthosilicate	$Si(OC_2H_5)_4$	AR	Sinopharm Chemical Reagent Co., Ltd.
Tetrabutyl titanate	$C_{16}H_{36}O_4Ti$	AR	Sinopharm Chemical Reagent Co., Ltd.
Phosphomolybdic acid	$H_3PMo_{12}O_{40}•xH_2O$	AR	Sinopharm Chemical Reagent Co., Ltd.
Phosphotungstic acid	$H_3PW_{12}O_{40}•xH_2O$	AR	Sinopharm Chemical Reagent Co., Ltd.
Ammonium molybdate	$(NH_4)_6Mo_7O_{24}$	AR	Sinopharm Chemical Reagent Co., Ltd.
Molybdenum trioxide	MoO_3	AR	Sinopharm Chemical Reagent Co., Ltd.
n-octane	C_8H_{18}	AR	Damao Chemical Reagent Factory
Benzothiophene	C_8H_6S	AR	Damao Chemical Reagent Factory
Dibenzothiophene	$C_{12}H_8S$	AR	Damao Chemical Reagent Factory
Sodium tungstate	$NaWO_4$	AR	Damao Chemical Reagent Factory
Tetrapropyl ammonium hydroxide	$C_{12}H_{29}NO$	AR	Energy Chemical
Silica sol	$SiO_2•xH_2O$	30%	Xinxing reagent Co., Ltd.
Hydrogen peroxide	H_2O_2	30%	Sinopharm Chemical Reagent Co., Ltd.
Phosphoric acid	H_3PO_4	AR	Energy Chemical

2.2. Preparation of catalysts

Preparation of TiO_2-SiO_2 nanocomposite oxide:

Method 1: According to the method in the literature[1], TEOS and anhydrous ethanol were uniformly mixed at a molar ratio of 1:5, and the mixture A was prepared after stirring for 1 h. Anhydrous ethanol, water, concentrated nitric acid, and TBOT were homogeneously mixed in a molar ratio of 30:300:1.8:1 and stirred for 1 h to make mixture B. The mixture was then mixed with water, nitric acid, and TBOT. Under vigorous stirring, the mixture B was added to the mixture A. The mixture was heated in a water bath at 50 ℃ for 2 h and then placed in an oven at 80 ℃ for 2 h. The obtained wet gel was vacuum dried at 100 °C for 6 h and then roasted at 400 °C for 6 h. The prepared catalyst was noted as TiO_2-SiO_2.

Method 2: Without the addition of H-β zeolite, the other steps were the same as those for the preparation of H-β@TiO_2@SiO_2-T+S. The catalyst produced was noted as TiO_2-SiO_2-T+S.

Table S2 The preparation methods of catalysts

catalyst	$m(SiO_2)$：m(H-β)	m(H-β)：m(TBOT)	reprocess
H-β-TPAOH@SiO_2	0.4：1		impregnation, drying, and roasting
H-β-TPAOH@TiO_2		1：2	impregnation, drying, and roasting
H-β@TiO_2@SiO_2-TS	0.4：1	1：2	impregnation, drying, and roasting
H-β@TiO_2@SiO_2-ST	0.4：1	1：2	impregnation, drying, and roasting
H-β@TiO_2@SiO_2-T+S	0.4：1	1：2	impregnation, drying, and roasting
H-β-TPAOH@TiO_2@SiO_2-TS	0.4：1	1：2	impregnation, drying, and roasting
H-β-TPAOH@TiO_2@SiO_2-ST	0.4：1	1：2	impregnation, drying, and roasting
H-β-TPAOH@TiO_2@SiO_2-T+S	0.4：1	1：2	impregnation, drying, and roasting

Note:(1) TS stands for titanium silylation followed by silanization, (2) ST stands for silanization followed by titanium silylation, (3) T+S stands for simultaneous titanium silylation treatment, (4) the catalysts in this chapter have the same designations as in this table.

Table S3 The preparation methods of POM/β-T+S and MoO_3/β-T+S

catalyst	m(POM)：m(T+S)	solvent	reaction temperature	reprocess
Keggin/β-T+S	1：20	water	room temperature	impregnation, drying, and roasting
Finke/β-T+S	1：20	water	120 °C reactor	impregnation, drying, and roasting
Anderson/β-T+S	1：20	water	120 °C reactor	impregnation, drying, and roasting
Dawson/β-T+S	1：20	water	120 °C reactor	impregnation, drying, and roasting
MoO_3/β-T+S	1：15	water	120 °C reactor	impregnation, drying, and roasting

Note：(1) Keggin includes HPW/HPMo；(2) Finke includes $Co_4(PW_9)_2$/$Zn_4(PW_9)_2$；(3) Anderson includes $FeMo_6$/AHM；(4) Dawson includes deletion type KP_2W_{17}/KP_2W_{18}.

2.4. Catalytic reaction

The sample conversion is expressed as X_{DS}, the initial oil sulfur mass fraction is denoted by ω, and the reacted oil sulfur mass fraction is denoted by ω_f in μg/g and is calculated as described below:

$$X_{DS} = \frac{\omega - \omega_f}{\omega} \times 100\%$$

3. Results and discussion

3.1. Catalysts characterization

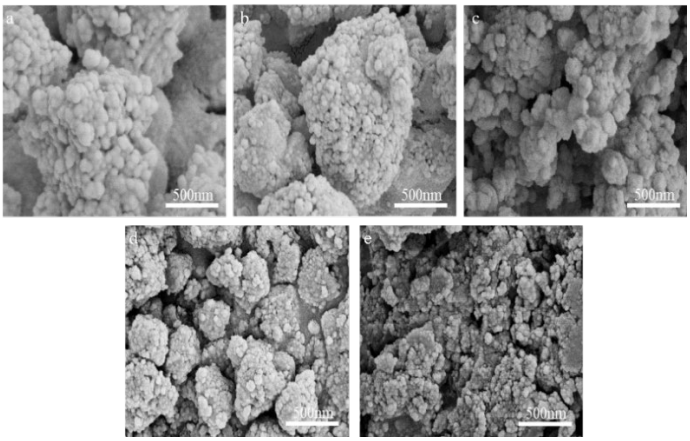

Fig.S1 SEM images of H-β zeolite and modified catalysts: (a) H-β, (b) H-β@TiO_2, (c) H-β-TPAOH, (d) H-β-TPAOH@TiO_2, (e) H-β-TPAOH@TiO_2@SiO_2-T+S.

The XRD patterns of H-β zeolite and the modified catalyst are shown in Fig.S2. By observing the patterns, it can be learned that there is no significant change in the structure of β-zeolite after modification. The diffraction peak position of β zeolite is consistent with the value in the standard card (# JCPDS 48-0074). And the diffraction intensity of the spectra decreased after the introduction of SiO_2, indicating a decrease in the crystallinity of the samples. The diffraction peaks at 2θ = 25.28 °, 37.78 °, 47.97 °, 53.79 ° and 62.70 ° correspond to the characteristic peaks of anatase TiO_2 (# JCPDS 21-1272). Compared with H-β-TPAOH@TiO_2, H-β-TPAOH@TiO_2@SiO_2-T+S has a lower crystallinity of anatase TiO_2[2].

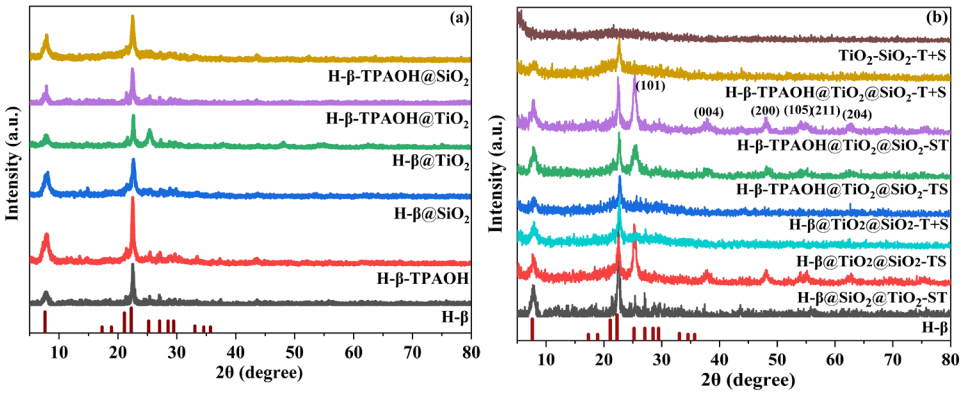

Fig.S2 XRD patterns of H-β zeolite and modified catalysts

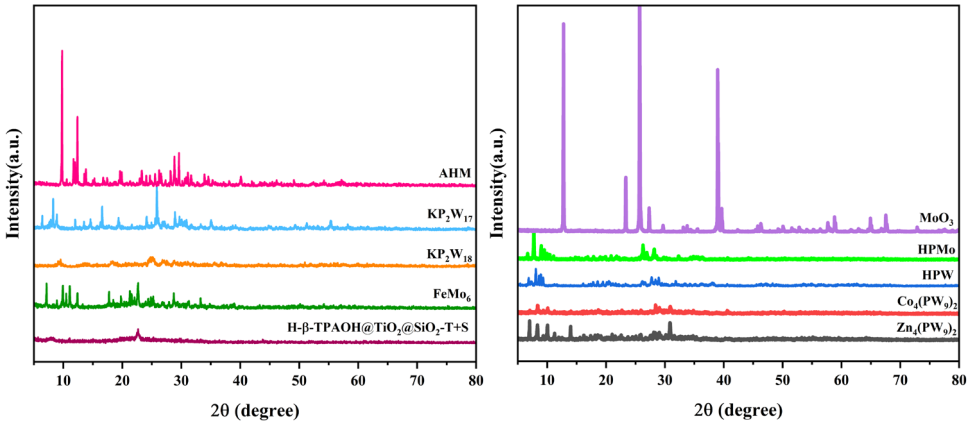

Fig.S3 XRD patterns of the support and the polyoxometalate parents

Fig. S4 shows the FT-IR spectra of the samples before and after the modification of nano-sized H-β zeolite. As can be seen from the figure, the H-β and modified zeolite can still be attributed to the characteristic bands of *BEA topology in the vicinity of 575 and 525 cm^{-1}. They are four-membered ring and double five-membered ring vibrations[3] and there is no significant change in the intensity compared to that before H-β modification. This indicates that the introduction of TiO_2 and SiO_2 and high-temperature roasting did not lead to significant changes in the backbone structure. Moreover, the alkali treatment, TiO_2 modification, SiO_2 modification, and the change in the modification order of H-β will not affect the structure of zeolite.

Fig.2(b) shows the FT-IR spectra of POM supported by β-T+S. In HPW/β-T+S, four characteristic vibration peaks belonging to the Keggin-type structure can be observed at 700~1100 cm^{-1}. The characteristic absorption bands near 1082 cm^{-1} (P-O), 980 cm^{-1} (W = Ot), 814 cm^{-1} (W-Oe-W) and 897 cm^{-1} (W-Ob-W) are consistent with the characteristic absorption bands of bulk HPW[4] which indicates that the Keggin structure is well retained in the prepared composites. The corresponding vibrational bands are slightly shifted, suggesting that the anions in HPW are chemically interacting with the β-zeolite surface. The characteristic vibrational peak at 780 ~ 1100 cm^{-1} has a very typical Keggin structure[5]. 1066 cm^{-1} is the asymmetric stretching vibration of P-Oa (Oa corresponds to the oxygen atom of the tetrahedral phosphate group), 966 cm^{-1} is the asymmetric stretching vibration of P-Oa Mo = Ot (Ot corresponds to the terminal oxygen atom), the bending vibration of Mo-Ob-Mo is 870 cm^{-1} (Ob corresponds to the oxygen atom bridging two tungsten atoms), and the bending vibration of Mo-Oc-Mo (Oc represents the oxygen atom on the Keggin structural angle) is 786 cm^{-1}. Among them, the characteristic peaks of HPMo at 791 and 1063 cm^{-1} overlap with the characteristic spectral bands of the *BEA structure, indicating that HPMo has been successfully loaded on the β-T+S support and still maintains its original structure on the support.

The polyanions of the Anderson structure $FeMo_6$, ammonium molybdate (referred to as HTP/AHM) at 869, 907, and 933 cm^{-1} correspond to vibrations of the terminal Mo=O group; the characteristic bands

of the bridged Mo-O-Mo bond at 603 and 648 cm^{-1} [6]; and 1467 cm^{-1} correspond to deformation oscillations of quaternary ammonium cations. The characteristic bands of POM with Dawson structure (vacant Dawson structure KP_2W_{17}, KP_2W_{18}) are at 900 ~ 1100 cm^{-1}, and at 780 cm^{-1} are bands (W-Oc-W), 911 cm^{-1} (W-Oe-W), 961 cm^{-1} (W = O), and 1087 cm^{-1} (P-O). The FT-IR results also prove that Dawson-type POM is successfully loaded onto the β-T+S support. The characteristic bands of Finke structure $Co_4(PW_9)_2$ and $Zn_4(PW9)_2$ appear in the symmetric stretching vibration of 982 cm^{-1} (W = O), and 956,888 and 826 cm^{-1} are W-Ot, corner-sharing (W-Ob), and edge-sharing (W-Oc), respectively[7], which proves that Finke-type POMs are also successfully loaded on the support β-T+S. The characteristic spectral bands of the MoO_3/β-T+S catalysts appear at 567, 858, and 997 cm^{-1} , which correspond to the Mo-O-Mo bending vibration, Mo-O-Mo vibration of Mo^{6+}, and terminal Mo=O stretching vibrational modes, respectively[8] . The strong peak at 605 cm^{-1} and the sharp peak at 489 cm^{-1} indicate the telescopic vibration of the oxygen atom in the Mo-O-Mo unit, and the vibration of the oxygen atom attaches to three molybdenum atoms, respectively[9].

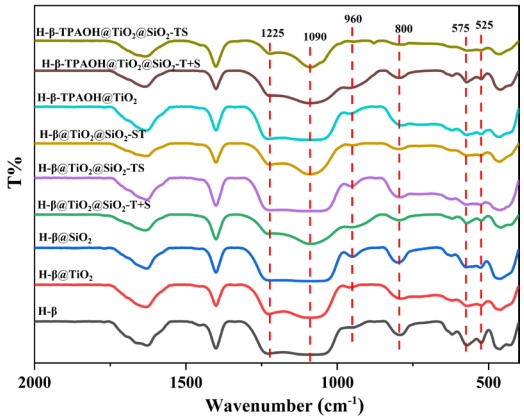

Fig. S4 FT-IR spectra of H-β zeolite and modified catalysts

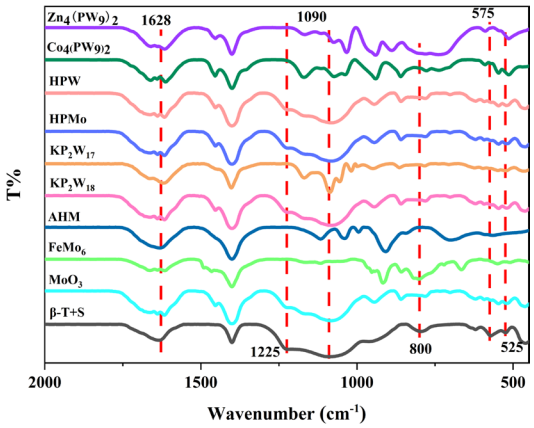

Fig.S5 FT-IR spectra of the support and the polyoxometalate parents

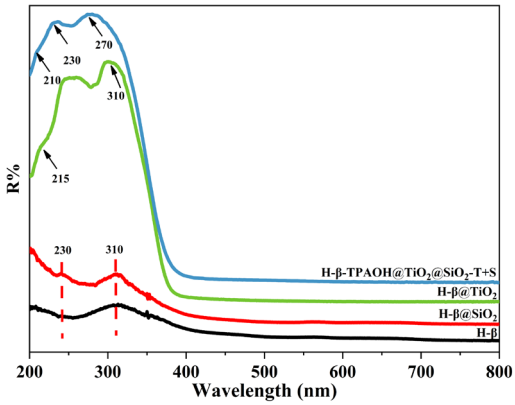

Fig. S6 UV-vis spectra of the samples before and after H-β zeolite modification

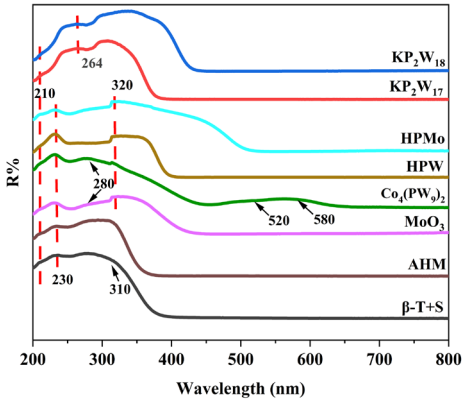

Fig.S7 UV-vis spectra of the support and the polyoxometalate parents

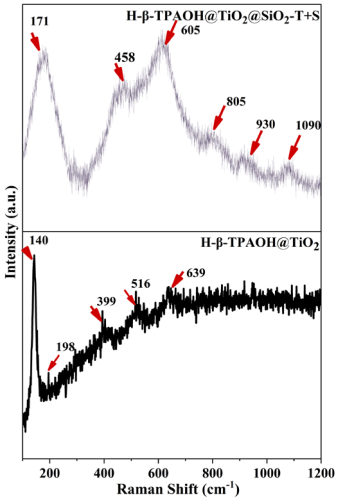

Fig. S8 Raman spectra of H-β-TPAOH@TiO_2 与 H-β-TPAOH@TiO_2@SiO_2-T+S samples

Table S4 The results of XRF

component	content
Al_2O_3	3.14
SiO_2	68.45
P_2O_5	0.18

	TiO_2	20.80
	WO_3	6.178

Table S5 The content of elements(EDX)

Elt.	Line	Intensity (c/s)	Conc	Units	Error 2-sig	MDL 3-sig	
C	Ka	75.40	23.112	wt.%	0.755	0.099	
O	Ka	208.84	37.599	wt.%	0.491	0.080	
Al	Ka	34.98	1.637	wt.%	1.566	0.038	
Si	Ka	572.02	25.822	wt.%	0.387	0.035	
Ti	Ka	102.72	9.006	wt.%	0.706	0.047	
W	La	2.28	2.825	wt.%	6.809	0.420	
			100.000	wt.%			Total

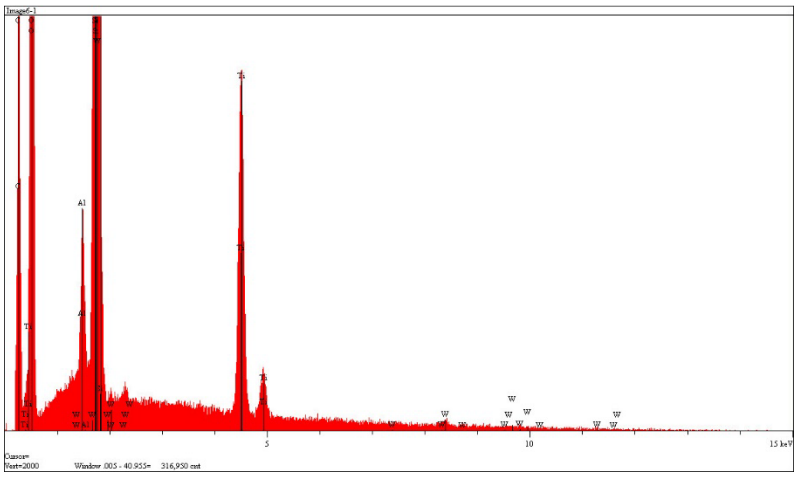

Fig. S9 EDX analysis of the HPW/β-T+S.

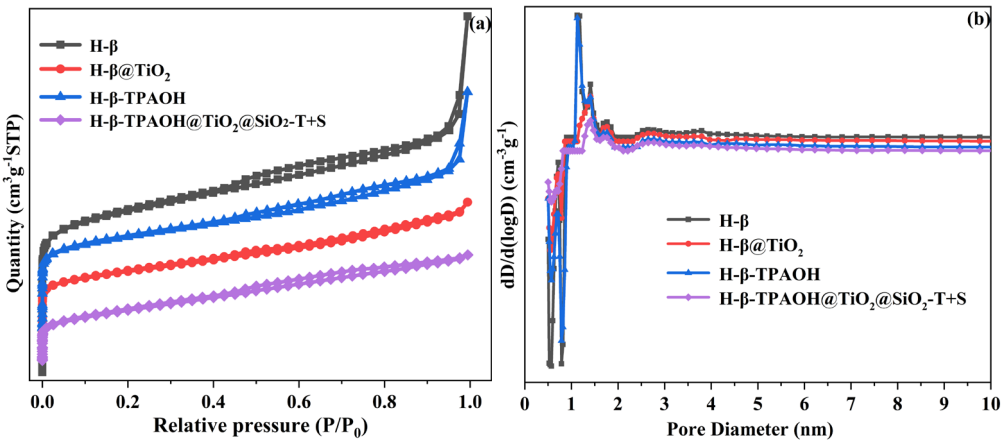

Fig. S10 N_2 adsorption-desorption isotherms and pore size distribution of samples

Table S6 The structure data of samples

Sample	S_{BET} (m^2/g)	Pore volume (cm^3/g)
H-β	563.6	0.59
H-β-TPAOH	505.1	0.62
H-β@TiO_2	382.6	0.35
H-β-TPAOH@TiO_2@SiO_2-T+S	304.2	0.28

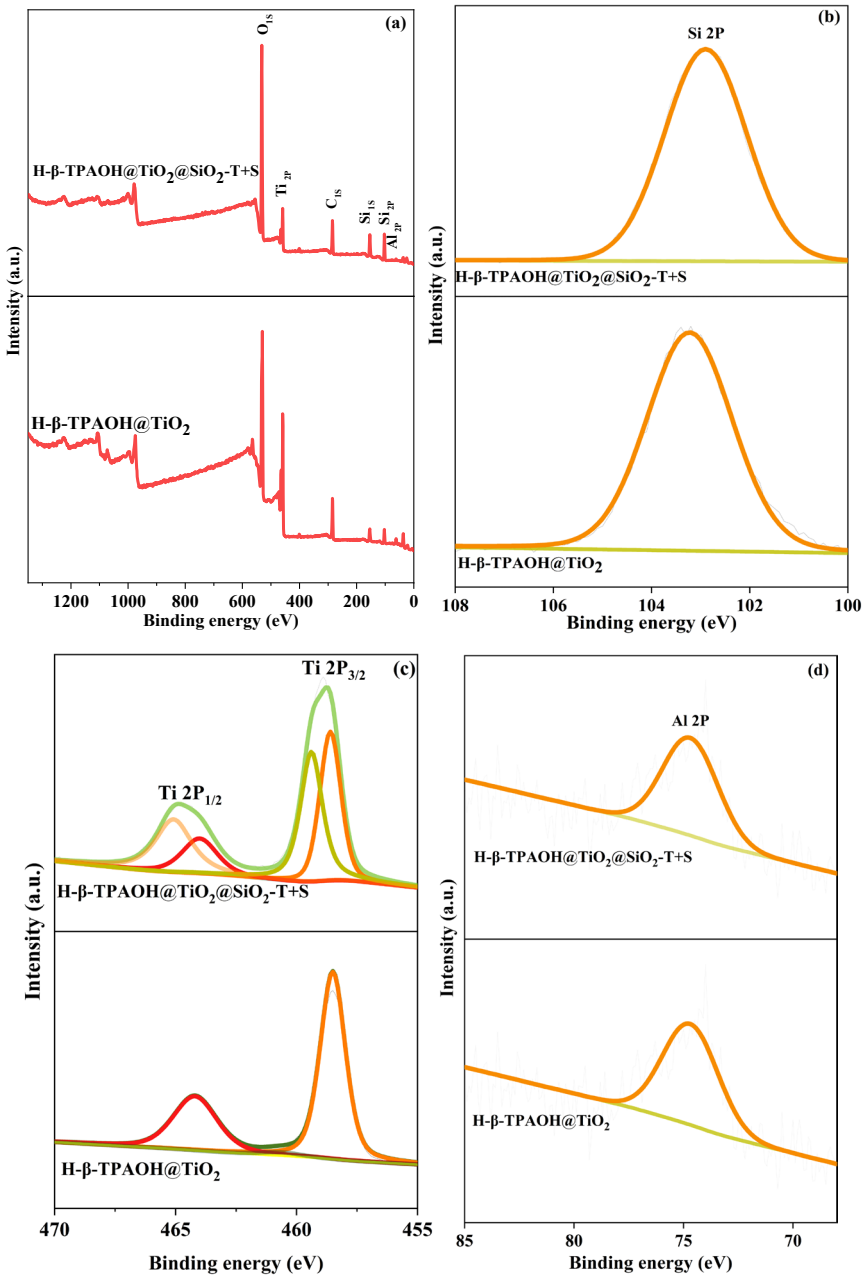

Fig.S11 XPS spectra of the same as above samples

Table S7 The content of Ti in different catalysts

catalyst	the content of Ti
H-β-TPAOH@TiO_2	33.5%
TPAOH@TiO_2@SiO_2-T+S	14.3%
HPW/β-T+S	11.2%
$Co_4(PW_9)_2$/β-T+S	9.6%
AHM/β-T+S	11.7%
KP_2W_{17}/β-T+S	14.0%
KP_2W_{18}/β-T+S	16.0%
MoO_3/β-T+S	14.6%

3.2. Evaluation of catalytic oxidation desulfurization performance

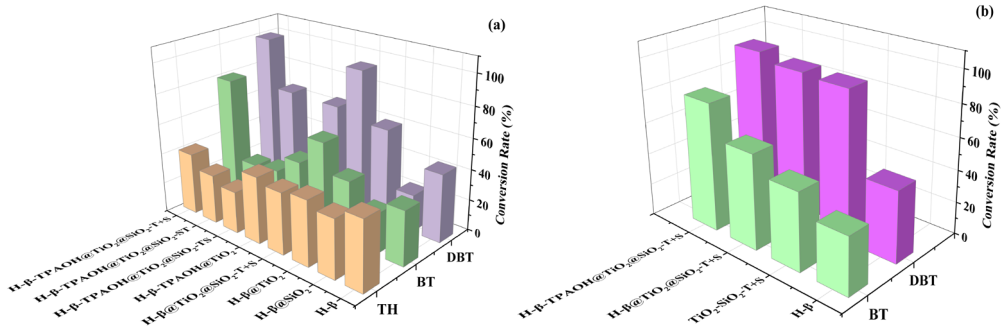

Fig.S12 Oxidative desulfurization performance of sulfur molecules over different catalysts

Table S8 The effect of different type of the catalyst on the ODS process

		Conversion rate			
entry	catalys	BT	DBT	time(min)	temperature(°C)
1	HPW/β-T+S	99.9	99.9	60	50
2	$PMnW_{11}$@PANI@CS	98	99	60	35
3	$(Gly)_3PMo_{12}O_{40}$@$MnFe_2O_4$	97.6	98.3	60	35
4	FWF@PbO@PVA	97	96	60	35

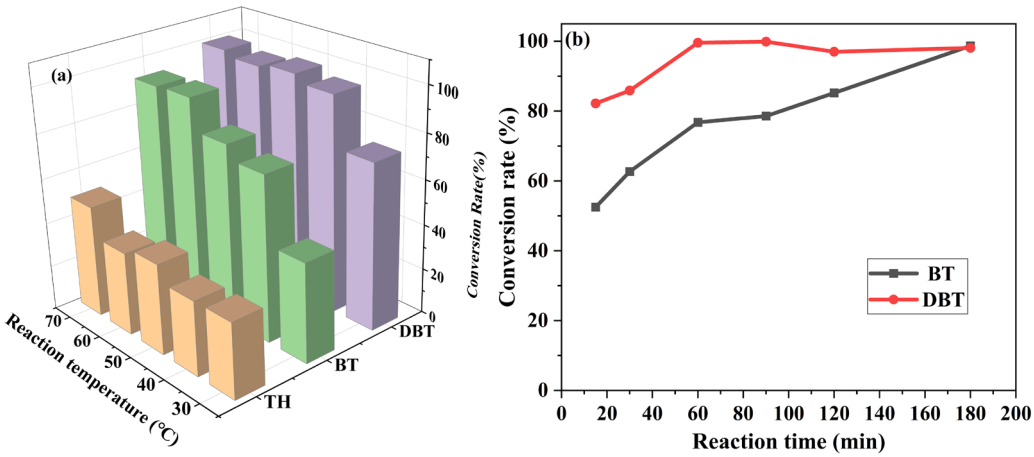

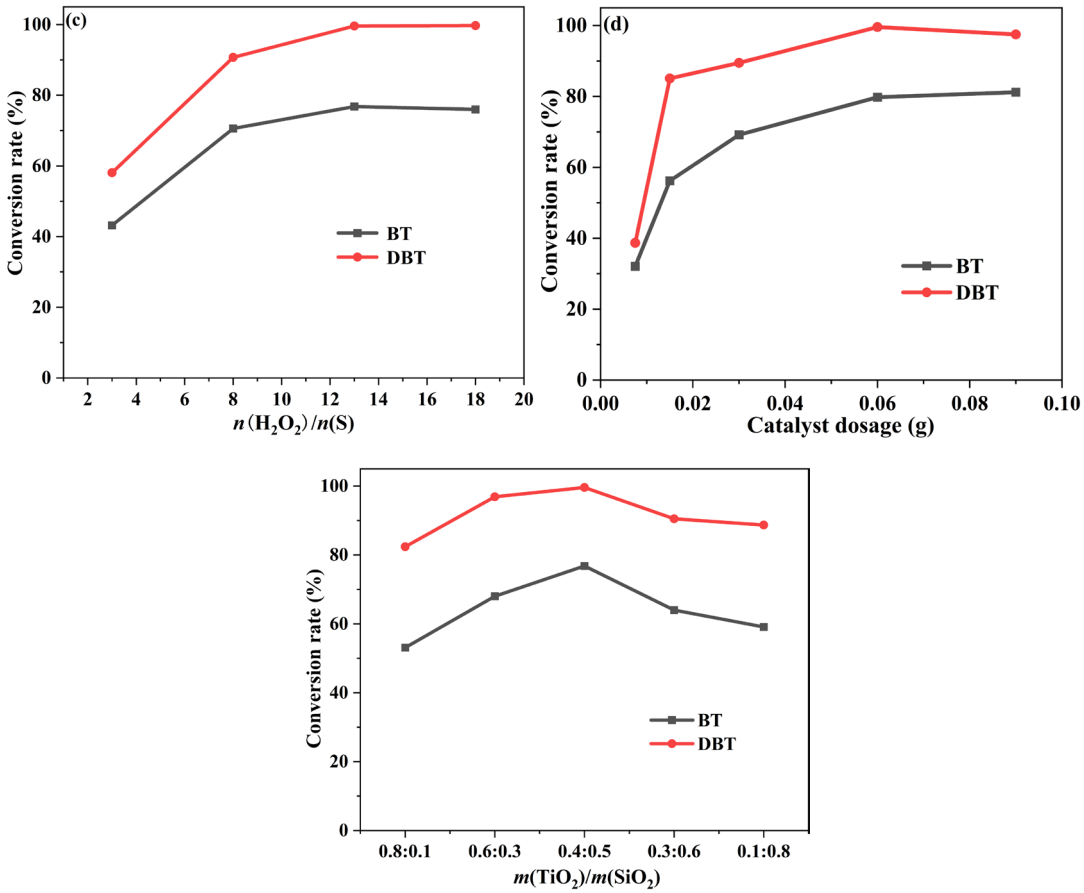

Fig.S13 The effect of reaction temperature, reaction time, oxidant dosage, catalyst dosage and Ti/Si ratios on the desulfurization performance of β-T+S

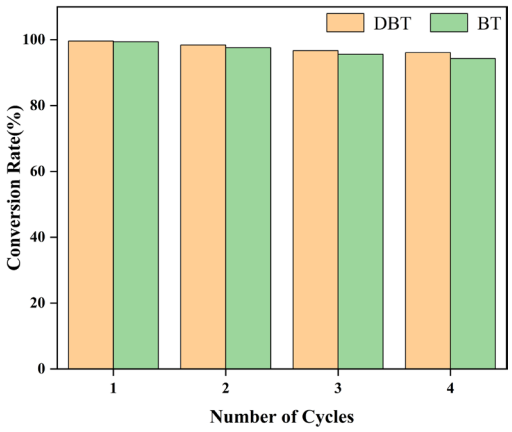

Fig.S14 The recycle of HPW/β-T+S

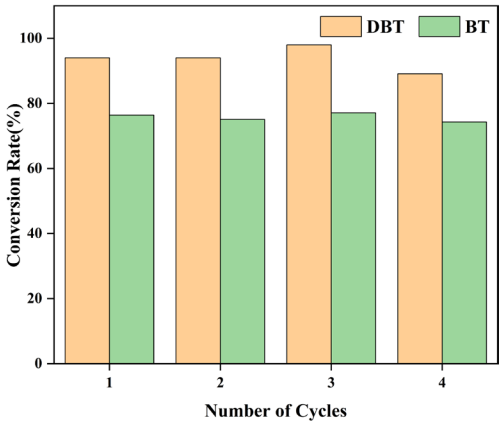

Fig.S15 The recycle of β-T+S

3.3. Discussion

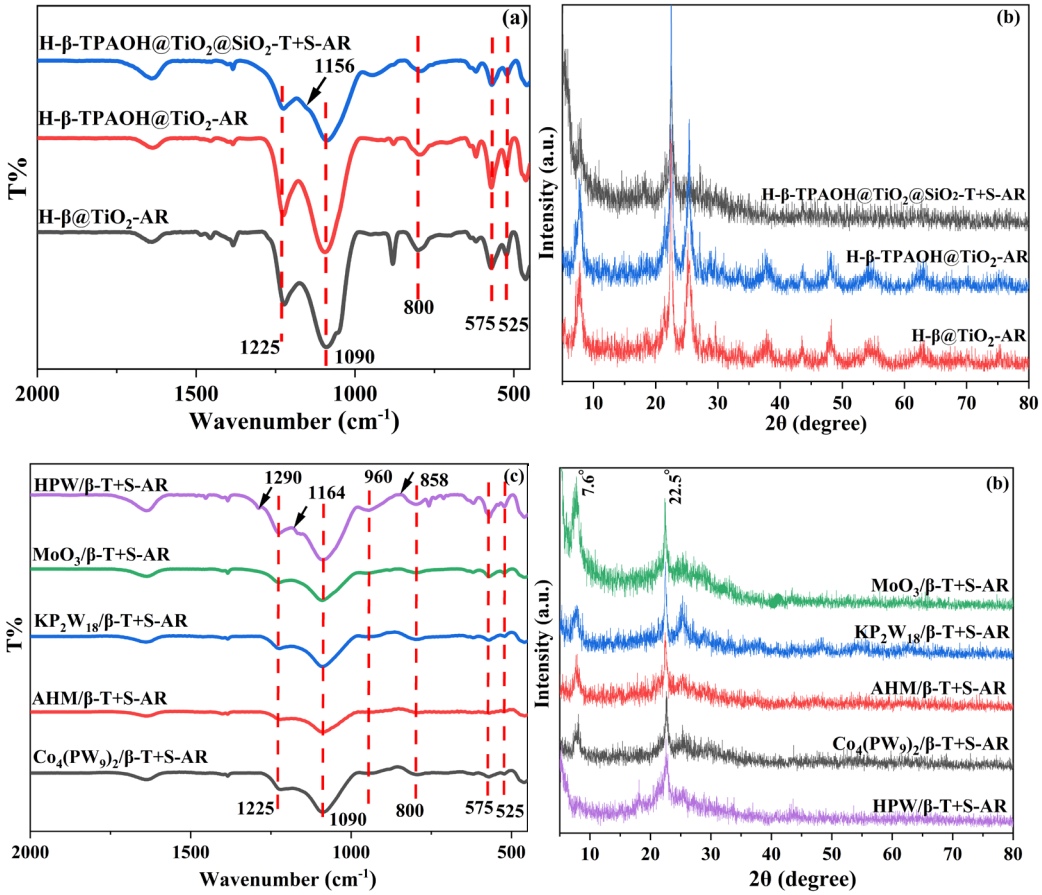

Fig.S16 FT-IR spectra and XRD pattern of samples after the reaction

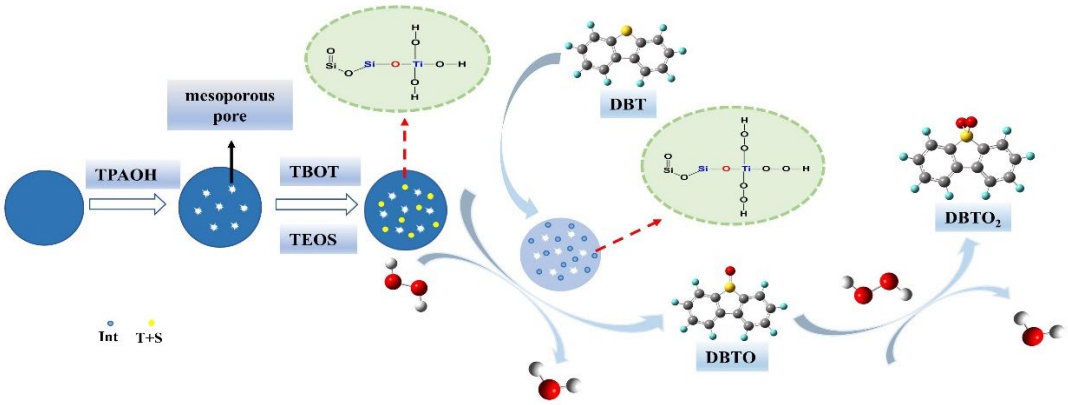

Fig.S17 The activation mechanism of ODS reaction over β-T+S catalyst.

Notes and references

1 A. Bazyari, A. A. Khodadadi, A. H. Mamaghani, J. Beheshtian, L. T. Thompson and Y. Mortazavi, *Appl. Catal. B*, 2016, **180**, 65-77.

2 M. Kobayashi, R. Kuma, S. Masaki and N. Sugishima, *Appl. Catal. B*, 2005, **60**, 173-179.

3 J. Perez-Pariente, J. A. Martens and P. A. Jacobs, *Applied Catalysis*, 1987, **31**, 35-64.

4 H. C. Gao, X. N. Wu, D. M. Sun, G. L. Niu, J. Y. Guan, X. F. Meng, C. Z. Liu, W. D. Xia and X. J. Song, *Dalton Trans.*, 2019, **48**, 5749-5755.

5 S. Farhadi, M. Hakimi and M. Maleki, *RSC Adv.*, 2018, **8**, 6768-6780.

6 J. H. Luo, Y. C. Huang, B. Ding, P. M. Wang, X. F. Geng, J. W. Zhang and Y. G. Wei, *Catalysts*, 2018, **8**, 121.

7 S. S. Balula, C. M. Granadeiro, A. D. Barbosa, I. C. Santos and L. Cunha-Silva, *Catal. Today*, 2013, **210**, 142-148.

8 S. W. Li, W. Wang and J. S. Zhao, *Appl. Catal. A-GEN*, 2020, **602**, 117671.

9 B. Gowtham, V. Ponnuswamy, G. Pradeesh, J. Chandrasekaran and D. Aradhana, *J. Mater. Sci. Mater. Electron.*, 2018, **29**, 6835-6843.